ANALYSIS OF THE LABORATORY IMPLEMENTATION OF A RADIAL ACTIVE MAGNETIC BEARING

Boštjan Polajžer[1], Drago Dolinar[1], Gorazd Štumberger[1], Oto Težak[1], Kay Hameyer[2]

[1] University of Maribor, Faculty of Electrical Engineering and Computer Science,
Smetanova 17, SI–2000 Maribor, Slovenia, *bostjan.polajzer@uni-mb.si*
[2] KU Leuven, Department E.E., Division ESAT/ELEN, Leuven, Belgium

Abstract ***– Stability and robustness of the controlled active magnetic bearings (AMB's), can be sufficiently improved with the knowledge of the mathematical model. Therefore an analysis of the laboratory implementation of a radial AMB is presented in the paper. The bearing force is determined by numerical calculations using 2D finite element method and the Maxwell's stress tensor. The current gain and position stiffness are determined in the entire operating range. The validation of the calculated bearing force, current gain and position stiffness is performed through the comparison with measured results. Moreover, the results of an approximation of the bearing force are presented. Obtained results make it possible to perform a robust control design in the entire operating range.***

Introduction

Magnetic bearings are technical applications of a stable rotor levitation. Various principles of magnetic bearings are known [1], but the principles based on controlled electro–magnetic circuits to provide the attractive force are the ones which are in common use. Two electromagnets on the opposite sides of the ferromagnetic rotor pull the rotor in the opposite direction. As such a system is unstable, a rotor position control is required to stabilize it. Bearings using this principle are called active magnetic bearings (AMB's). Due to their non-contact operation, AMB's offer significant advantages. Higher speed, no friction, no lubrication, precise position control and active vibration damping make them particularly appropriate for high–speed rotating machines. Technical applications include pumps, centrifuges and precise machine tools.

Stability and robustness of the controlled AMB's must be achieved in the entire operating range. To design a low order robust controller only relevant and possible model uncertainties should be taken into account. Therefore a careful analysis of the magnetic bearing must be performed, using the finite element method (FEM) and measurements [2, 3].

In this work, an analysis of the laboratory implementation of AMB's is presented (Fig. 2). The bearing force is a non-linear function of the currents and the rotor position. Therefore, the differential driving mode and the linearization of the bearing force are performed. The current gain and position stiffness are defined as partial derivatives of the bearing force. Furthermore, the FEM procedure for the force determination is described. The force is calculated by the Maxwell's stress tensor method using the programming environment described in [4]. The validation of the calculated bearing force and the data fitting are performed through the comparison with measured forces. The current gain and position stiffness are determined in the entire operating range. Thus, the mathematical model of the magnetic bearing is known in the entire operating range, but only relevant and possible model uncertainties are considered. Moreover, an analytical description of the mathematical model is presented approximating the bearing force. Using this results the robust low order controller, valid in the entire operating range, will be designed in the next step of this development.

Laboratory Implementation of Active Magnetic Bearings

The discussed system of AMB's is presented in Fig. 2. It is highly simplified, consisting of a pair of radial magnetic bearings placed at one end of the shaft and a ball bearing placed at the other end. Each of the magnetic bearing is used to stabilize the shaft movement only in one direction, i.e. the horizontal and vertical direction. The rotor and the four–pole stator are made out of laminated steel. Windings are connected in series and supplied in such a way that they can be considered as two "horse–shoe" electromagnets, as shown in Fig. 1.

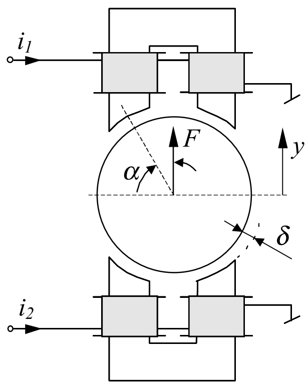

Fig. 1. Schematic presentation of a radial magnetic bearing

In the mathematical modeling of the radial magnetic bearing the rotation of the rotor and the non-linear iron properties are neglected, while windings of all electromagnets are assumed to be ideal and identical. In equation (1) the non-linear dependence of the resultant electromagnetic force F on the currents of both electromagnets i_1 and i_2 and the rotor position y is expressed. δ denotes the nominal air gap, while k represents the material and geometrical properties.

$$F(i_1, i_2, y) = k\left(\frac{i_1^2}{(\delta - y)^2} - \frac{i_2^2}{(\delta + y)^2}\right) \tag{1}$$

$$i_1 := i_0 + i_\Delta; \qquad i_1 := i_0 - i_\Delta \tag{2}$$

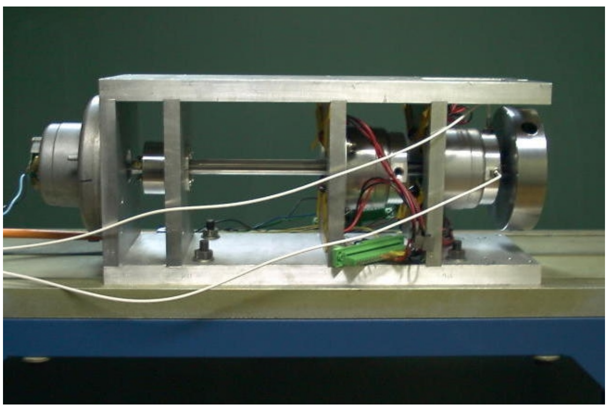

Fig. 2. Laboratory implementation of AMB's

With the introduction of the differential driving mode (2), a bias current i_0 is operating the winding of both electromagnets. Force control is performed by superposing a control current i_Δ to the winding of one electromagnet and subtracting it in the winding of other one, where $i_\Delta \leq i_0$. In spite of constant losses due to the bias current the chosen driving mode is justified, since the force–current dependence becomes linear for small rotor displacements. In addition, equation (1) is linearized considering the differential driving mode. The obtained equation (3) is valid in the vicinity of the operating point ($i_{\Delta OP}$, y_{OP}), whereby the current gain k_i and position stiffness k_y are defined by (4). If we want to consider the influence of non-linear iron properties, local saturations and magnetic flux leakage, we have to use FEM-based numerical calculations.

$$F(i_\Delta, y) = F(i_{\Delta OP}, y_{OP}) + k_i (i_\Delta - i_{\Delta OP}) + k_y (y - y_{OP}) \tag{3}$$

$$k_i := \left.\frac{\partial F(i_\Delta, y)}{\partial i_\Delta}\right|_{OP} ; \qquad k_y := \left.\frac{\partial F(i_\Delta, y)}{\partial y}\right|_{OP} \tag{4}$$

Force Calculation

In this section the procedure for calculating the force of the radial magnetic bearing is presented. The geometry and data of the laboratory implementation of a radial magnetic bearing are presented in Fig. 3 and in Table 1. The FEM-based calculation is implemented in the programming environment, which is described in [4]. The calculation for the chosen points (i_Δ, y) is carried out in four steps.

- **Step 1:** Task definition. The bearing geometry, the material, the current densities, and the boundary conditions are parametrically defined.

- **Step 2:** The initial discretization of the model is performed. The largest element's edge is explicitly defined for the air gap region. In this way the classical mesh adaptation is avoided, which reduces the calculation time by 40%.

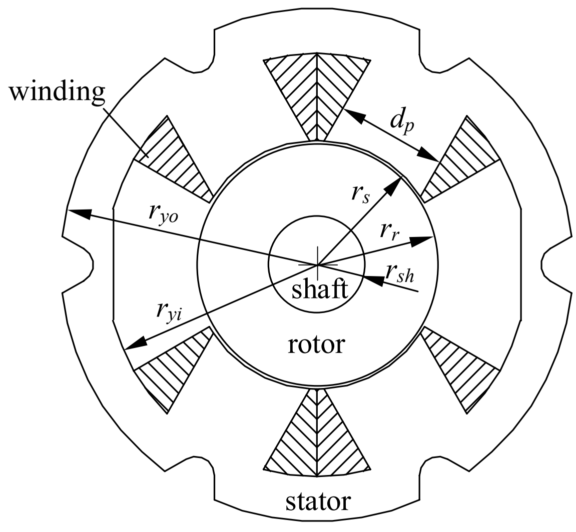

Fig. 3. Geometry of the radial magnetic bearing

Table 1. Data of the radial magnetic bearing

data	parameter	value
shaft radius	r_{sh} [mm]	8.00
rotor radius	r_r [mm]	19.25
stator radius	r_s [mm]	19.85
yoke inner radius	r_{yi} [mm]	33.80
yoke outer radius	r_{yo} [mm]	41.00
pole width	d_p [mm]	17.80
bearing length	l [mm]	30.70
angle between two poles	2α [rad]	π/3
number of turns per pole	$N/2$	50
bias current	i_0 [A]	2.5

• **Step 3:** The non-linear solution of the magnetic vector potential **A** is obtained by means of 2D computation based on the FEM. The problem is formulated by Poisson's equation (5), where ν represents the magnetic reluctance, **J** is the current density vector, and ∇ is Hamilton's differential operator.

$$\nabla \cdot (\nu \nabla \mathbf{A}) = -\mathbf{J} \qquad (5)$$

• **Step 4:** The force is determined by Maxwell's stress tensor **T**, following equation (6). Vector **F** consists tangential and normal force component, **n** is the unit normal vector of the integration surface *S*. In the 2D case the integration is performed over the contour placed exactly in the middle of the air gap.

$$\mathbf{F} = \nu \oint_S \mathbf{T}\,\mathbf{n}\, dS \qquad (6)$$

Force Measurement

The validation of the calculated force is performed by measurements. Force is measured via a handle–lever that connects the shaft and the bending beam. The position of the rotor is measured by an induction proximity probe, while each electromagnet is separately supplied by a DC current. Before starting with measurements the initial shaft position point, i.e. the center of the bearing ($y = 0$) must be found. After determining the center we start with force measurements in chosen points (i_Δ, y). In this procedure the forces for all selected control currents are measured at all rotor positions.

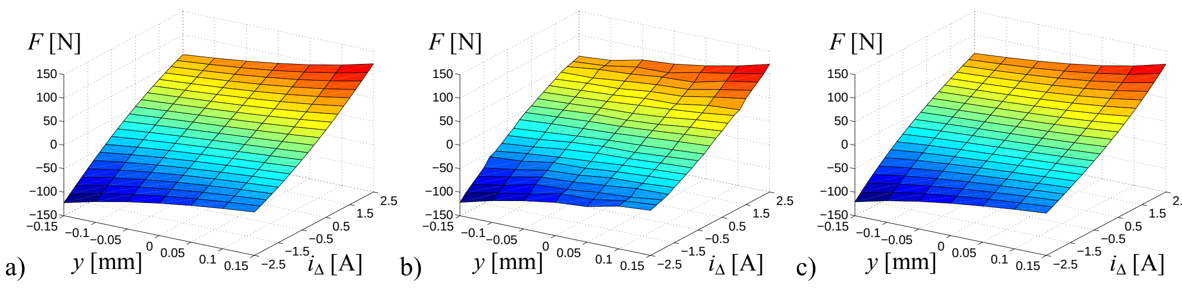

Fig. 4. Force F(i_Δ, y): a) FEM, b) measurements, c) approximation function of measured results

Results

The numerical calculation of the bearing force is highly dependent on the air gap. Due to the manufactured rotor steel sheets the magnetic active air gap is bigger than the geometric air gap. Therefore, data fitting is considered in the force calculation. In our case the air gap is increased from 0.6mm to 0.663mm. In the FEM procedure the rotor radius is varied until the calculation agrees with measured value for the typical case (i_Δ = 1A, y = 0mm). Since results of the calculation in all other points of the operating range agree with measurements, this approach can be accepted. The increase in the air gap for 0.063mm can be compared with the findings of authors in [3]. The agreement between calculated and measured force (Figs. 4a,b) is very good. The maximum difference reaches 8N, but the average relative difference is below 7.4%.

We determine the current gain k_i as the quotient of the force difference and control current difference, and the position stiffness k_y as the quotient of the force difference and rotor position difference in the entire operating range. The results of the differentiation of calculated and measured results are quite close and are shown in Figs. 5a,b) and 6a,b).

To obtain an analytical description of the bearing force we present the measured force with an approximation function (7), which is shown in Fig. 4c). Thus, it is possible to determine k_i and k_y as an analytical current and position derivatives of the function (7) respectively (Figs. 5c, 6c).

$$\begin{aligned} F(i_\Delta, y) = & -\left(88.65\, e^{-0.2170\, y} + 0.26\, e^{-15.1085\, y}\right) e^{\left(1267.26\, e^{-0.9724\, y} - 1267.44\, e^{-0.9727\, y}\right) i_\Delta} + \\ & + \left(1.75\, e^{8.9870\, y} + 86.69\, e^{0.4413\, y}\right) e^{\left(616.66\, e^{1.1180\, y} - 616.48\, e^{1.1176\, y}\right) i_\Delta} \end{aligned} \tag{7}$$

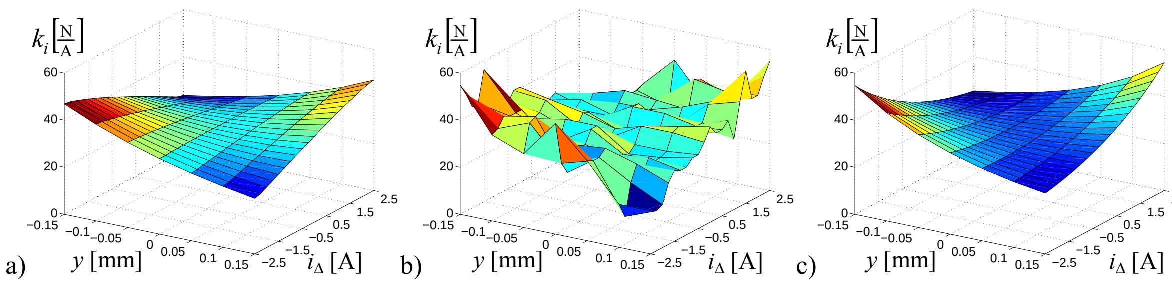

Fig. 5. Current gain k_i: a) differentiation of the FEM-based results, b) differentiation of measured results, c) analytical derivation of the approximation function

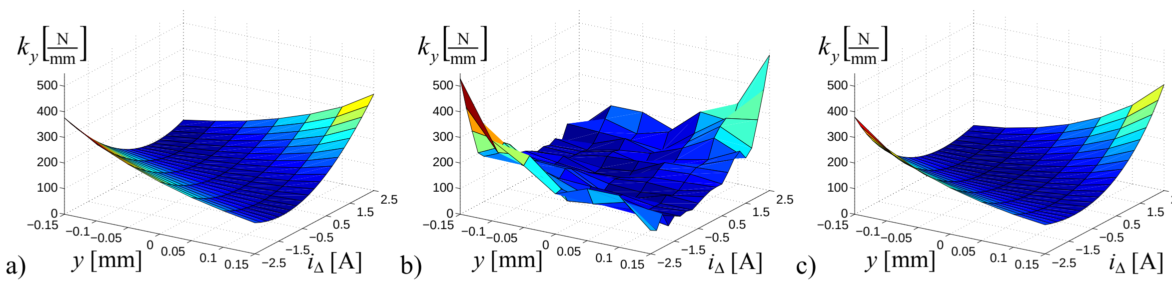

Fig. 6. Position stiffness k_y: a) differentiation of the FEM-based results, b) differentiation of measured results, c) analytical derivation of the approximation function

Conclusion

An analysis of the laboratory implementation of AMB's is presented in the paper. The linearized force expression of the bearing is written, by defining the current gain and the position stiffness. The force is determined by FEM-based calculations using the Maxwell's stress tensor. To update the model uncertainties the data fitting is used in the calculation procedure. The validation of the calculated force is performed by measurements. The agreement between calculated and measured force is very good. Differentiation of the bearing force is used to determine the current gain and position stiffness in the entire operating range. Obtained results determine the mathematical model in the entire operating range including only relevant and possible model uncertainties. To obtain an analytical description of the mathematical model an approximation of the bearing force is performed. This results make it possible to perform a robust control design in the entire operating range and will be applied in the next step of the development of the AMB.

References

[1] G. Schweitzer, H. Bleuler and A. Traxler, *Active magnetic bearings*. ETH Zürich: Vdf Hochschulverlag AG an der ETH Zürich, 1994.

[2] G. Štumberger, D. Dolinar, U. Pahner and K. Hameyer, "Optimization of radial active magnetic bearings using the finite element technique and the differential evolution algorithm," *IEEE Transaction on Magnetics*, vol. 36, no. 4, pp. 1009–1013, 2000.

[3] M. Antila, E. Lantto and A. Arkkio, "Determination of forces and linearized parameters of radial active magnetic bearings by finite element technique," *IEEE Transaction on Magnetics*, vol. 34, no. 3, pp. 684–694,1998.

[4] U. Pahner, R. Mertens, H. D. Gersem, R. Belmans and K. Hameyer, "A parametric finite element environment tuned for numerical optimization," *IEEE Transaction on Magnetics*, vol. 34, no. 5, pp. 2936–2939, 1998.